



Aptamer-based fluorometric lateral flow assay for creatine kinase MB

Jing Zhang¹ · Xuefei Lv¹ · Wei Feng¹ · Xiaoqiong Li¹ · Kunjie Li¹ · Yulin Deng¹

Received: 23 April 2018 / Accepted: 28 June 2018 / Published online: 7 July 2018
© Springer-Verlag GmbH Austria, part of Springer Nature 2018

Abstract

A group of aptamers possessing high specificity and affinity for creatine kinase MB (CKMB) was obtained by magnetic systematic evolution of ligands by exponential enrichment. Two aptamers (referred to as C.Apt.21 and C.Apt.30) were found to possess adequately low K_d values. They form a well suited pair for CKMB binding. By using fluorescent microspheres, an aptamer-based lateral flow assay was developed. It is portable, economical, and sensitive. The limit of detection for CKMB is as low as $0.63 \text{ ng}\cdot\text{mL}^{-1}$, and the assay works in the $0.005 - 2 \text{ }\mu\text{g}\cdot\text{mL}^{-1}$ CKMB concentration range. The method is specific for CKMB, and biomarkers for AMI (such as cardiac troponin I and myoglobin) and serum do not interfere. The strip is highly accurate as shown by analysis of spiked serum samples which gave recoveries ranging between 88 and 117%.

Keywords CKMB · Aptamer · Magnetic SELEX · Lateral flow · Fluorescent microsphere · Nanoparticles · Rapid detection · Test strip reader · Sandwich · Acute myocardial infarction

Introduction

Acute myocardial infarction (AMI) is one of the leading life-threatening diseases in the world with high incidence and death rate [1, 2]. The rapid and accurate prediction, diagnosis, and prognosis of AMI are of significant importance. The MB isoform of creatine kinase (CKMB) is a biomarker for the diagnosis of AMI [3]. Sequential measurements of CKMB have been demonstrated to be useful for monitoring reinfarction [4].

Enzyme-linked immunosorbent assays (ELISAs) and radioimmunoassay (RIAs) are often used for monitoring CKMB levels in clinical diagnosis and treatment [5, 6]. But ELISAs requires a relatively long time for detection (over 6 h), and requires well-trained staffs to operate [7]. Lateral flow test strips have been used as powerful tools for biomarker detec-

tion. It is a point-of-care testing method which can be performed without a skilled technician [9].

Colloidal gold is first applied to lateral flow assay (LFA). The experimental results can be observed visually. Colloidal gold-based LFA has been previously used for the detection of human $\text{IFN}\gamma$ [8]. Mao et al. [10] used a rapid quantitative immunochromatographic strip for simultaneous detection of multiple proteins. Ang et al. [11] also developed a gold nanoparticle-based sandwich immunoassay for the dual detection and measurement of hemoglobin A1c (HbA1c) and total hemoglobin. By comparison, fluorescent microspheres (FMs), a type of polystyrene material, can generate stable fluorescence. FMs have the advantages of stable morphology, durable light excitation, uniform particle size, high biocompatibility, good dispersibility, and modifiable surfaces [12, 13]. FMs can be used in LFA for qualitative and quantitative detection. Some of the most important indicators for evaluating the performance of biomarker assays are sensitivity and reproducibility [14]. Therefore, the fluorescent microsphere lateral flow assay (FM-LFA) can be used as a useful tool for improving the sensitivity and reproducibility of rapid biomarker assays. For example, Wang et al. [12] used FM-LFA for detecting fumonisin B1 (FB1). Chen et al. [13] developed a FM-LFA for the determination of sulfamethazine (SMZ) in milk.

Electronic supplementary material The online version of this article (<https://doi.org/10.1007/s00604-018-2905-4>) contains supplementary material, which is available to authorized users.

✉ Xiaoqiong Li
aeople@126.com

¹ Beijing Key Laboratory for Separation and Analysis in Biomedicine and Pharmaceuticals, School of Life Science, Beijing Institute of Technology, 5 South Zhongguancun Street, Haidian District, Beijing 100081, People's Republic of China

The above methods are based on antigen–antibody interactions. Antibodies have disadvantages such as high production cost, low stability at high temperatures, and difficult chemical modifications. Because of similar recognition properties, aptamers have been proposed as a potential substitute for conventional antibodies [15]. In addition, aptamers are low cost, chemically stable, and easy to modify. The use of aptamers as alternatives to antibodies in test strip methods has been demonstrated to yield satisfactory results [16, 17], Mao et al. [17] used aptamers in LFA for target DNA detection for the first time. Overall, we hypothesize that CKMB can be detected using an aptamer sandwich lateral flow assay.

A matched fluorescent LFA analytic device is pivotal for quantitative detection of the test strips. And it is expected to make major contributions to point-of-care testing in the future [18]. Establishing a fluorescent test strip reader is necessary to achieve lower LOD and reduce sample amount under different quantification criteria [19]. The test strip reader is used for measurements of fluorescence intensity. The intensities are recorded by a suitable software. The procedure includes placing a test strip under the camera and dropping a controlled amount of monochromatic light on the observed areas. The wavelength of light can be adjusted to achieve a good contrast between test and control lines and background. Automated systems are more favorable than manual processing in adjusting variables and handling results. Most studies involving fluorescent LFA used universal UV-light or fluorescence microscopes as simple detectors [20, 21]. However, these laboratory methods require a high investment, large space, and skilled technicians. These are disfavor the uses of test strip. Several other image sensor-based methods, such as the charge coupled device [22], complementary metal oxide semiconductor [23], and smartphone camera [24, 25] were developed in resolving the issues aforementioned. But their deficiencies in sensitivity reflected in the signal-to-noise ratio persist. The design of a fluorescent test strip reader is very important for the high sensitivity and quantitative detection in fluorescent microsphere lateral flow assays.

Here, single-stranded DNA (ssDNA) aptamers with high affinity and specificity to CKMB were selected by systematic evolution of ligands by exponential enrichment (SELEX) [26]. A sandwich aptamer-based LFA was developed. A newly portable, economical, and sensitive fluorescent LFA analytical device was designed. Qualitative and quantitative detection of CKMB was realized.

Experimental

In vitro selection of the specific aptamers for CKMB

Aptamers for CKMB were selected using the magnetic SELEX method developed in our group [27] with minor modification (See [Electronic Supplementary Material](#), ESM).

Estimation of dissociation constant (Kd) by enzyme-linked aptamer assay

All of the sequenced aptamers were synthesized. The dissociation constant (Kd) was assayed using an enzyme-linked aptamer assay (See ESM). Dissociation constants were calculated by nonlinear regression curve fitting using GraphPad Prism, with the one site binding (hyperbolic) equation $Y = \frac{B_{max} \cdot X}{Kd + X}$. Y represents the mean value of OD 450 nm. Bmax is the maximal value of OD 450 nm. X is the concentration of the aptamer (0 – 400 nM).

Preparation and characterizations of FM-C.Apt.30 conjugates

The streptavidin-fluorescent microparticles and biotinylated aptamer C.Apt.30 were used for the preparation of FM-C.Apt.30 conjugates, through streptavidin-biotin interaction. Briefly, 0.1 mg of FMs diluted in 500 μ L of 10 mM phosphate buffered saline (PBS, 20 mM $\text{NaH}_2\text{PO}_4 \cdot \text{H}_2\text{O}$, 80 mM $\text{Na}_2\text{HPO}_4 \cdot 2\text{H}_2\text{O}$, 137 mM NaCl, pH 7.4) were centrifuged at 17,000 g at 4 $^\circ\text{C}$ for 30 min to wash the FMs. The sediment was resuspended in 500 μ L of 10 mM phosphate buffered saline (PBS). Then, 50 pmol of C.Apt.30 was added to the suspension and incubated for 30 min at room temperature. FM-Apt conjugates were centrifuged at 17,000 g at 4 $^\circ\text{C}$ to remove any unbound aptamers. Next, FM-C.Apt.30 conjugates were blocked with 250 μ L of 10 mM phosphate buffered saline (PBS) containing 10 mM biotin for 30 min at room temperature. The mixture was centrifuged at 17,000 g for 30 min. The final FM-C.Apt.30 conjugates were dissolved in 250 μ L of 10 mM phosphate buffered saline (PBS) containing 10 mM biotin. The FM-C.Apt.30 conjugates were stored at 4 $^\circ\text{C}$ until use. FMs and FM-C.Apt.30 conjugates were analyzed using the multi-mode microplate reader.

Preparation of test strips

As shown in Fig. 1a, the structure of the test strips was composed of a sample pad, absorbent pad, and a NC membrane. All parts were pasted on a PVC backing card. Before assembly, the sample pad and NC membrane were preprocessed. The sample pad was saturated for 30 min with 10 mM phosphate buffered saline (PBS) containing 0.1% Tween 20 (v/v) and 1% BSA (w/v), then dried at room temperature for overnight and preserved in a sealed bag. Next, the streptavidin-C.Apt.21 conjugates at a concentration of 1 OD/30 μ L were immobilized on the NC membrane as a test line. 0.25 OD/30 μ L of streptavidin-DNA probe conjugates were immobilized as a control line. The solution for the dilution of streptavidin-aptamer/DNA probe conjugates were 10 mM phosphate buffered saline (PBS). The NC membrane with lines were dried at ambient temperature for 10

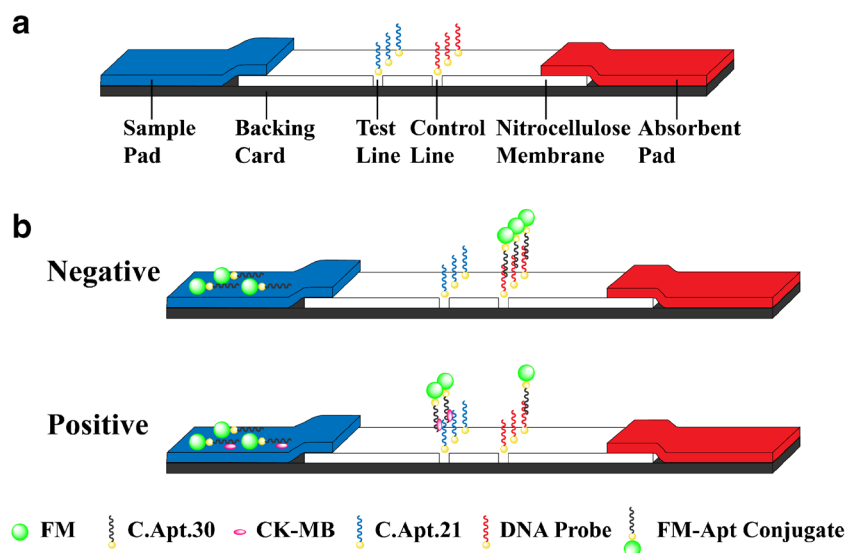


Fig. 1 Schematic illustration of the test strip (a) and the principle of fluorescent microsphere lateral flow test strip assay based on sandwich aptamers for CKMB detection (b). In the absence of CKMB (negative), FM-C.Apt.30 conjugates move along the nitrocellulose membranes by capillary action and are captured by the DNA probe immobilized on the

control line (C line). In the presence of CKMB (positive), CKMB is bound with FM-C.Apt.30 conjugates. The FM-C.Apt.30-CKMB complex is captured by C.Apt.21 immobilized on the test line (T line), and the unreacted FM-C.Apt.30 conjugates are captured by the DNA probe immobilized on the control line (C line)

min. After assembly, it was cut into 4-mm strips and stored at room temperature in a sealed bag.

Design of the test strip reader

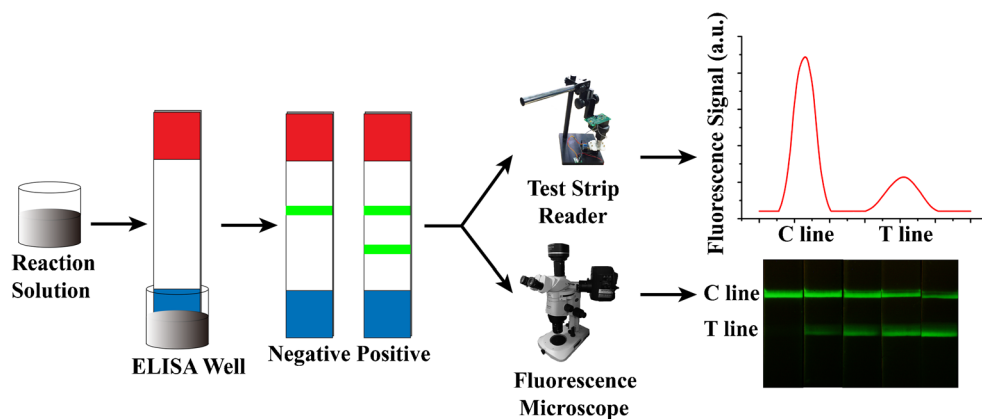
An analytical device was designed herein for fluorescence signal detection and data processing. Shown in Figure S4B is a picture for the test strip reader. A high-powered LED with a wavelength of 470 nm (LDW5SM-4S4T-35, Osram) was chosen as the excitation light source. The corresponding optical paths for fluorescence detection was based on the excitation and emission of co-linear optical paths (Figure S4A). The optical path was divided into two parts: excitation and emission. The excitation light path comprised an excitation light filter (470 ± 10 nm, Bodian Optical, China), a planoconvex lens (LA1805, Thorlabs, USA), a reflection of a dichroic mirror (cut-off at 509 nm, Bodian Optical, China), and an objective lens (PLL 20X, Cossim, China). The excitation light was illuminated onto the fluorescent lines (T line and C line) on the test strip. FMs on the lines were excited, emitting light with a wavelength peak of 530 nm. The emission light path comprised an objective lens, a transmission of a dichroic mirror, an optical filter (530 ± 10 nm, Bodian Optical, China), and a planoconvex lens. Next, the emission light was focused on the photo-sensing surface of monolithic photodiode (OPT101, Texas Instruments) and sampled by an analog-digital converter (AD7734, Analog Devices). Then the data was transmitted to a microcontroller unit (MSP430-F5636, Texas Instruments) that communicated with the computer by an Ethernet interface. Ultimately, a master computer software based on an area

algorithm was used to process chromatographic peak data and generated a result report. In order to ensure the stability of the test, a stepper motor (28BYJ-48, Telesky, China) was used as a mechanical sliding structure to ensure the automation and stability of the test. Then, the strip with a shell was inserted to touch the shrapnel. Finally, the enabling signal was automatically triggered.

Fluorescence assay procedure

As illustrated in Fig. 2, the fluorescence assay procedure is as follows: first, 100 μ L of reaction solution including FM-C.Apt.30 conjugates, samples, detergent (Tween 20), and 10 mM phosphate buffered saline (PBS) was mixed in the ELISA well. Then, a test strip was inserted into this reaction solution at room temperature for 10 min. The reaction solution flowed through the NC membrane via capillary action. For the detection of CKMB in the serum, 20-fold phosphate buffered saline (PBS) diluted artificial serum spiked. Different amounts of CKMB was added onto the reaction buffer. After 10 min, by using the test strip reader, FMs were excited by a 470-nm laser diode. The fluorescence signals were transferred to the computer and processed by software. Then, the fluorescence peak area intensity of the control line (FI_C) and the fluorescence peak area intensity of test line (FI_T) were obtained. Imaging can also be performed by placing the test strip under a fluorescence microscope with an excitation wavelength of 470 nm. Under the same conditions, each sample was tested three times.

Fig. 2 Schematic illustration of the detection procedure



Statistical analysis

Data were analyzed statistically by one-way analysis of variance (ANOVA) using SPSS16.0 statistical software. All data points were based on at least three duplicate experiments. Significant differences between groups were assessed by ANOVA combined with least significant difference post-hoc tests. Data were calculated as means \pm SD ($n = 3$). In pairwise comparisons, a value of $p > 0.05$ represents no significant difference. A value of $p < 0.05$ represents significant. A value of $p < 0.01$ represents highly significant. A value of $p < 0.001$ represents very highly significant.

Results and discussion

In vitro selection of aptamers for CKMB

The enrichment of CKMB aptamers were monitored by a direct enzyme-linked assay. The amounts of ssDNA specifically bound to CKMB were characterized by the absorbance at 450 nm of the final products in each well. The results are shown in Figure S1. From rounds 1 to 10, the absorbance increases. The affinity of the ssDNA pools increases during the progression of the magnetic SELEX. As shown in results of the one-way ANOVA, the affinities of the ssDNA pools for CKMB increase significantly ($p < 0.001$). The least significant difference post hoc test shows the difference significant mean between each round between rounds 1–9 ($p < 0.05$). On the contrary, the absorbance decreases significantly from rounds 1 to round 2 ($p < 0.05$), and is maintained at a low level in the negative group (myoglobin). In the blank group (BSA only), the absorbance is very low from rounds 1 to 10. All of the results demonstrate the magnetic SELEX enriching ssDNA. ssDNA shows an affinity for CKMB.

The DNA pool generated after round 10 was cloned and sequenced. Randomized parts of sequences identified were aligned with CLUSTAL X. All of the identified sequences

of aptamers are shown in Table S1. The percentages of guanine are relatively high (more than 50%). The G-quartets in 10 sequences were analyzed by QGRS Mapper (Table S2). Except for C.Apt.16, the other aptamers shows a potential to fold into one (or two) G-quartet. As the result indicated, the G-quartet is the basic structure for the interaction between the aptamer and CKMB. In other studies, the G-quartet also plays a pivotal role in the binding mechanism of aptamers with the ligand [28, 29].

Characterization of the CKMB aptamer candidates

The dissociation constants were calculated by the nonlinear regression equation (Figure S2). All K_d values are listed in Table S1. The K_d values of the aptamers range from 0.81 to 272 nM. The K_d values herein are at the same level with those of other studies that used an enzyme-linked aptamer assay to determine K_d values [30, 31]. Combined with the results of aptamer sequences and K_d values, 4 sequences, C.Apt.1, C.Apt.3, C.Apt.21, and C.Apt.30 have more higher affinity and stable G-quarter structure. These 4 sequences were chosen for further study.

Longer aptamer chains results in higher experimental cost. In order minimize costs, the primer domains at the two sides of C.Apt.1, C.Apt.3, C.Apt.21 and C.Apt.30 were shortened. Their K_d values were determined to evaluate the effect on the specificity and affinity of aptamers with CKMB. As shown in Figure S3, shortened C.Apt.1, C.Apt.3, C.Apt.21 and C.Apt.30 is bound to CKMB with K_d values of 63.57 ± 6.86 nM, 35.21 ± 4.45 nM, 14.74 ± 1.86 nM and 24.04 ± 4.50 nM, respectively. From the results, the shortened aptamers still possess high specificity and affinity with CKMB. They can be used in subsequent studies. And the affinities of shortened aptamer C.Apt.21 and C.Apt.30 are higher than that of C.Apt.1 and C.Apt.3. The shortened aptamer C.Apt.21 and C.Apt.30 were chosen for further study.

Design of the fluorescent microsphere lateral flow assay (FM-LFA)

Figure 1b shows the principle of the assay. It is based on the specific affinity between CKMB and selected aptamers to form a sandwich structure (C.Apt.30-CKMB-C.Apt.21). In the presence of CKMB, C.Apt.30 and FM conjugates (FM-C.Apt.30) capture CKMB to form FM-C.Apt.30-CKMB complexes. By using the capillary effect, complexes flow along the NC membrane. Then they were capture by the C.Apt.21 immobilized on the test line. Excited at a wavelength of 470 nm, the complexes emit fluorescence on the test line. The greater the amount of CKMB present in the reaction solution, the stronger the fluorescence emit on the test line. On the contrary, when CKMB is absent, no complex is formed on the test line with no fluorescence emitted after excitation. Regardless, DNA probes immobilized on the control line can capture excess FM-C.Apt.30 to ensure the validity of the test strip.

For the quantitative detection of CKMB, taking into account the environmental and matrix factors may affecting the intensity of the fluorescence signal, the FI_T/FI_C ratio was used to counteract the intrinsic non-uniformity of the test strip [32].

Characterization of fluorescent microspheres (FMs) and their Apt conjugates

The successful coupling of FMs to the aptamer is one of the most important steps. It usually affects the results of CKMB determination. The coupling of FMs with aptamer herein is based on biotin-avidin system. It is more convenient and effective than coupling of FMs with antibodies. The FM-C.Apt.30 conjugates were characterized by fluorescence. As shown in Fig. 3, the maximal emission peak. Apt.30 conjugates are similar to that of free FMs. Their maximal emission are all around 484 nm. But the fluorescence intensity of the FM-C.Apt.30 conjugates is lower than that of free FMs. It

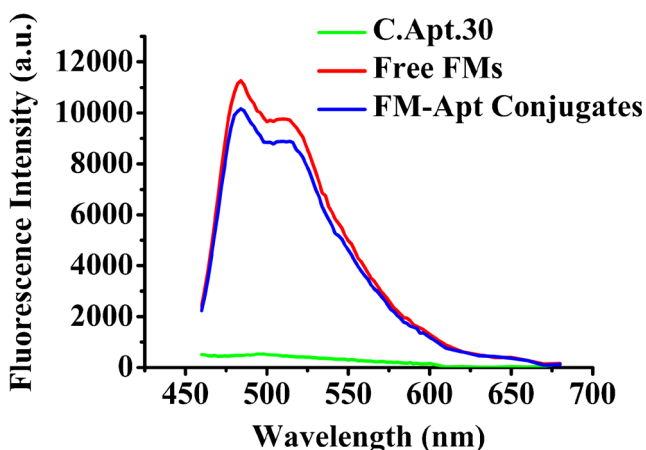


Fig. 3 Fluorescence spectrum (excitation wavelength = 425 nm) of C.Apt.30, free FMs, and FM-C.Apt.30 conjugates

might be caused by the attachment of aptamers with FMs, blocking parts of fluorescences. This result indicates the aptamer bound to FMs successfully. The result is similar to that of Liu et al. [33]. As shown in result of Liu et al. [33], the antibody on the FM surface can shield a portion of the fluorescence signal.

Optimization of method

The following parameters were optimized: (a) Composition of the coupling buffer; (b) Amount of FM-C.Apt.30 conjugates and C.Apt.30; (c) Type and percentages of the detergent; (d) The concentration of DNA probe on the control line and C.Apt.21 on the test line. Respective data and Figures are given in the [Electronic Supplementary Material](#). The following experimental conditions were found to give best results: (a) Composition of the coupling buffer: phosphate buffered saline (PBS); (b) Optimal amount of FM-C.Apt.30 conjugates and C.Apt.30: 4 μg and 0.05 nmol; (c) Type and percentages of the detergent: Tween 20 and 1%; (d) Optimal

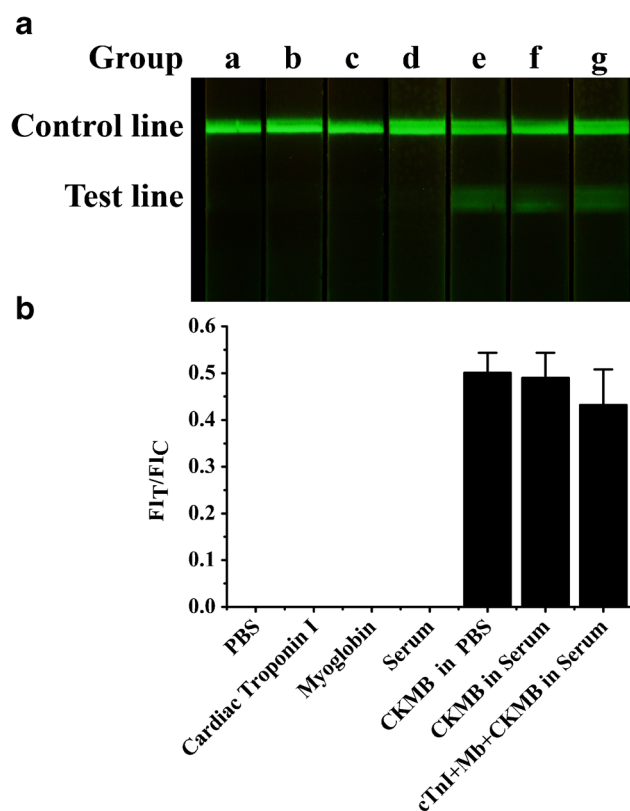
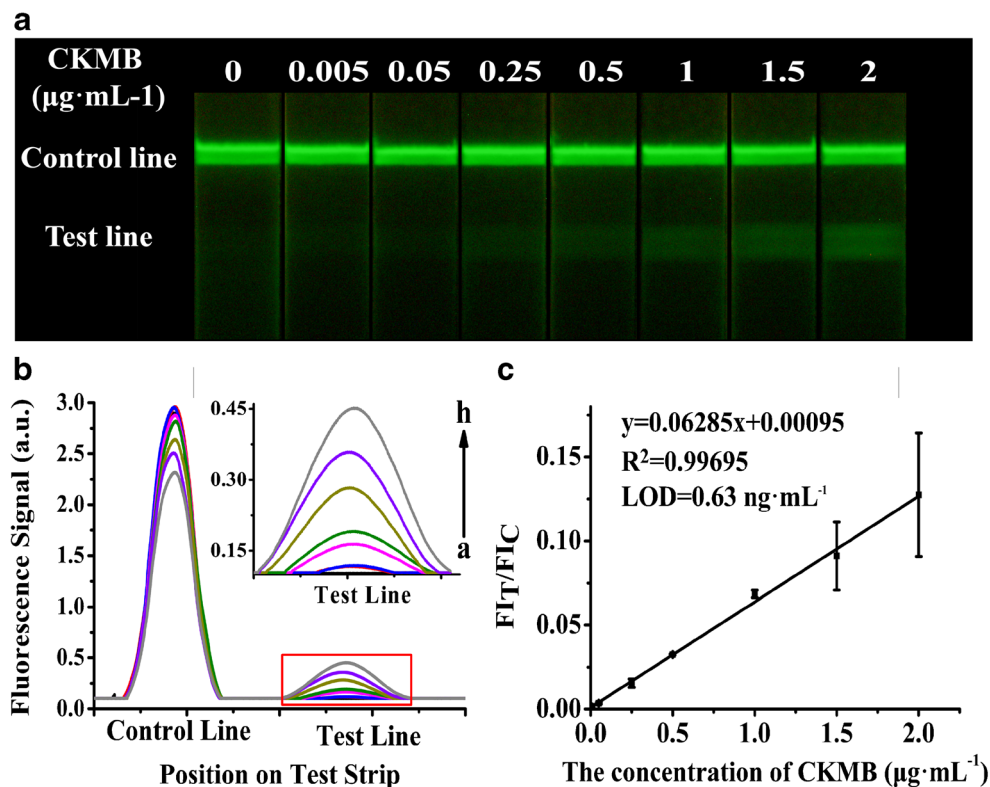


Fig. 4 Specificity analysis of the fluorescent microsphere lateral flow test strip assay. **a** Pictures of the test strips under a fluorescence microscope. **b** FI_T/FI_C ratio by test strip reader. All values are means \pm SD ($n = 3$). And “a” represents blank with phosphate buffered saline (PBS) buffer, “b” represents 2 $\mu\text{g}\cdot\text{mL}^{-1}$ cTnI (Cardiac Troponin I) in PBS buffer, “c” represents 2 $\mu\text{g}\cdot\text{mL}^{-1}$ myoglobin in PBS buffer, “d” represents serum, “e” represents 2 $\mu\text{g}\cdot\text{mL}^{-1}$ CKMB in PBS buffer, “f” represents 2 $\mu\text{g}\cdot\text{mL}^{-1}$ CKMB in serum, “g” represents 2 $\mu\text{g}\cdot\text{mL}^{-1}$ cTnI, 2 $\mu\text{g}\cdot\text{mL}^{-1}$ myoglobin and 2 $\mu\text{g}\cdot\text{mL}^{-1}$ CKMB in serum

Fig. 5 The quantitative detection and qualitative analysis of CKMB by fluorescent microsphere lateral flow test strips with a series of spiked concentrations (0, 0.005, 0.05, 0.25, 0.5, 1, 1.5, and 2 $\mu\text{g}\cdot\text{mL}^{-1}$) in artificial serum. **a** Pictures of the test strips obtained under a fluorescence microscope for qualitative analysis. **b** Fluorescence responses by test strip reader for (a) 0 $\mu\text{g}\cdot\text{mL}^{-1}$, (b) 0.005 $\mu\text{g}\cdot\text{mL}^{-1}$, (c) 0.05 $\mu\text{g}\cdot\text{mL}^{-1}$, (d) 0.25 $\mu\text{g}\cdot\text{mL}^{-1}$, (e) 0.5 $\mu\text{g}\cdot\text{mL}^{-1}$, (f) 1 $\mu\text{g}\cdot\text{mL}^{-1}$, (g) 1.5 $\mu\text{g}\cdot\text{mL}^{-1}$, and (h) 2 $\mu\text{g}\cdot\text{mL}^{-1}$ CKMB, respectively. **c** Calibrated curve for quantitative detection of CKMB. All values are means \pm SD ($n = 3$)



concentration of DNA probe and C.Apt.21: 0.25 OD/30 μL and 1 OD/30 μL .

Specificity of the fluorescent microsphere lateral flow assay (FM-LFA)

Cardiac troponin I (cTnI) and myoglobin (Mb) were used as the negative control group. Phosphate buffered saline (PBS) and artificial serum were used as the blank control group. 2 $\mu\text{g}\cdot\text{mL}^{-1}$ CKMB in phosphate buffer, 2 $\mu\text{g}\cdot\text{mL}^{-1}$ CKMB in serum, and the mixture of 2 $\mu\text{g}\cdot\text{mL}^{-1}$ cTnI, 2 $\mu\text{g}\cdot\text{mL}^{-1}$ Mb, and 2 $\mu\text{g}\cdot\text{mL}^{-1}$ CKMB in serum were used as the test group. As shown in Fig. 4, for the test group, obvious fluorescent bands in the test and control zones are observed. The FI_T/FI_C ratios of the test groups are significantly higher than those in the

negative and blank control groups. There is no significant difference ($p > 0.05$) between CKMB in phosphate buffered saline (PBS) and serum. It further indicates that serum does not interfere the detection of CKMB. Furthermore, there is also no significant difference ($p > 0.05$) between CKMB in phosphate buffered saline (PBS) and mixture in serum, indicating the great specificity of FM-LFA. As shown in these results, FM-LFA has high specificity for CKMB detection, and other AMI biomarkers and serum don't cause the interference.

Quantitative evaluation of the assay

Under the optimized condition, the method was used to quantitatively detect CKMB. As shown in Fig. 5a, the test strips with different concentrations of CKMB (0, 0.005, 0.05, 0.25,

Table 1 The accuracy and precision of FM-LFA for detection of CKMB spiked in serum

CKMB ($\mu\text{g}/\text{mL}$)	Intra-assay				Inter-assay			
	Mean ($\mu\text{g}/\text{mL}$)	SD	Recovery (%)	CV (%)	Mean ($\mu\text{g}/\text{mL}$)	SD	Recovery (%)	CV (%)
0.5	0.44	0.02	88.0	3.8	0.51	0.04	102.0	7.9
1.0	0.95	0.02	95.0	1.6	1.00	0.09	100.0	9.0
2.0	2.10	0.07	105.0	3.2	2.34	0.12	117.0	5.2

All values are means \pm SD ($n=3$)

0.5, 1, 1.5, and 2 $\mu\text{g}\cdot\text{mL}^{-1}$) are observed under an Olympus microscope with an excitation wavelength of 470 nm. The results indicated that with an increase in CKMB concentration, fluorescence intensity on the test and control lines are enhanced and reduced, respectively. However, only the concentration of CKMB is higher than 0.25 $\mu\text{g}\cdot\text{mL}^{-1}$, the fluorescence intensity on the test line can be observed by an Olympus microscope digital camera. At the same time, the test strips with different concentrations of CKMB from 0 to 2 $\mu\text{g}\cdot\text{mL}^{-1}$ (curve a–h) are also detected by our designed test strip reader (Fig. 5b). As can be seen from the figure, the peak area of the test line increases with increasing concentrations of CKMB, while the peak area of the control line decreases. Moreover, the fluorescence signal of CKMB of 0.005 $\mu\text{g}\cdot\text{mL}^{-1}$ can be detected by the test strip reader. This demonstrates that the designed test strip reader possesses perfect sensitivity for fluorescent signals. The calibration curve was obtained by recording the FI_T/FI_C ratio of different CKMB concentrations (0.005, 0.05, 0.25, 0.5, 1, 1.5, and 2 $\mu\text{g}\cdot\text{mL}^{-1}$) serially diluted in serum. As indicated in Fig. 5c, the regression equation can be fit into a polynomial as $y = 0.00095 + 0.06285x$ with $R^2=0.99695$, where x is the concentration of CKMB, y is the FI_T/FI_C ratio, and R is the regression coefficient. The LOD was calculated to be 0.63 $\text{ng}\cdot\text{mL}^{-1}$ by analyzing a zero calibrator 20 times. The LOD is lower than 0.8 $\text{ng}\cdot\text{mL}^{-1}$. Furthermore, 0.8 $\text{ng}\cdot\text{mL}^{-1}$ is also the LOD for CKMB in the study of Torabi et al. [14], who utilized a chemiluminescence immunoassay based on ELISA.

Detection of real samples

The accuracy and precision of the fluorescent microsphere lateral flow assay (FM-LFA) were also evaluated by detecting CKMB spiked serum samples, and the recovery was calculated. Low (0.5 $\mu\text{g}\cdot\text{mL}^{-1}$), medium (1.0 $\mu\text{g}\cdot\text{mL}^{-1}$), and high concentrations (2.0 $\mu\text{g}\cdot\text{mL}^{-1}$) of CKMB were spiked in artificial serum samples for analysis. The intra-assay recoveries are 88.0, 95.0, and 105.0%, and the inter-assay recoveries are 102.0, 100.0, and 117%, respectively. The average recovery is 101.2%. The coefficient of variation is between 1.6 to 9.0% (Table 1). These results indicate that the accuracy of FM-LFA is acceptable for the quantitative detection of CKMB.

Conclusions

In this study, ssDNA for the AMI biomarker CKMB were screened by magnetic SELEX. Based on these aptamers, a double aptamer sandwich LFA was developed. Combined with the designed test strip reader, the fluorescent microsphere lateral flow assay can be used for fast detection of CKMB. This method only identifies CKMB. As a result, CKMB is detected at a concentration of 0.63 $\text{ng}\cdot\text{mL}^{-1}$ in serum. This

limit of detection is lower than cutoff value of CKMB (5 $\text{ng}\cdot\text{mL}^{-1}$) for AMI. In order to apply the platform to the clinical diagnosis of AMI, we have to overcome the influence of whole blood to binding between aptamer and targets. In further studies, the target-specific aptamer assay is expected to become a valuable platform for various diseases diagnosis. But because of the limited availability of aptamer types, aptamer-based assays are still immature when compared to immunoassays. We wish that aptamer will become a useful tool in target detection that could meet challenges.

Acknowledgement This work was partly supported by the National Special R&D Programmer for Key Scientific Instruments and Equipment (2012YQ04014001) and the Beijing Institute of Technology Research Foundation (3160050321211).

Compliance with ethical standards The author(s) declare that they have no competing interests.

References

1. WHO (2014) Cardiovascular diseases. http://www.who.int/cardiovascular_diseases/en/
2. Thygesen K, Alpert JS, White HD (2007) Universal definition of myocardial infarction. *Circulation* 116(22):2634–2653. <https://doi.org/10.1161/CIRCULATIONAHA.107.187397>
3. Lai XH, Liang RL, Liu TC, Dong ZN, Wu YS, Li LH (2016) A fluorescence immunochromatographic assay using europium (III) chelate microparticles for rapid, quantitative and sensitive detection of creatine kinase MB. *J Fluoresc* 26(3):987–996. <https://doi.org/10.1007/s10895-016-1786-3>
4. Friess U, Stark M (2009) Cardiac markers: a clear cause for point-of-care testing. *Anal Bioanal Chem* 393(5):1453–1462. <https://doi.org/10.1007/s00216-008-2573-z>
5. Roberts R, Sobel BE, Parker CW (1976) Radioimmunoassay for creatine kinase isoenzymes. *Science* 194(4267):855–857
6. Hammerer-Lercher A, Erlacher P, Bittner R, Korinthenberg R, Skladal D, Sorichter S, Sperl W, Puschendorf B, Mair J (2001) Clinical and experimental results on cardiac troponin expression in Duchenne muscular dystrophy. *Clin Chem* 47(3):451–458
7. Zhang GJ, Ning Y (2012) Silicon nanowire biosensor and its applications in disease diagnostics: a review. *Anal Chim Acta* 749:1–15. <https://doi.org/10.1016/j.aca.2012.08.035>
8. Chou SF (2013) Development of a manual self-assembled colloidal gold nanoparticle-immunochromatographic strip for rapid determination of human interferon-gamma. *Analyst* 138(9):2620–2623. <https://doi.org/10.1039/c3an36547f>
9. Li X, Li W, Yang Q, Gong X, Guo W, Dong C, Liu J, Xuan L, Chang J (2014) Rapid and quantitative detection of prostate specific antigen with a quantum dot nanobeads-based immunochromatography test strip. *ACS Appl Mater Interfaces* 6(9):6406–6414. <https://doi.org/10.1021/am5012782>
10. Mao X, Wang W, Du T-E (2013) Rapid quantitative immunochromatographic strip for multiple proteins test. *Sensors Actuators B Chem* 186:315–320. <https://doi.org/10.1016/j.snb.2013.05.083>
11. Ang SH, Rambeli M, Thevarajah TM, Alias YB, Khor SM (2016) Quantitative, single-step dual measurement of hemoglobin A1c and total hemoglobin in human whole blood using a gold sandwich immunochromatographic assay for personalized medicine.

- Biosens Bioelectron 78:187–193. <https://doi.org/10.1016/j.bios.2015.11.045>
12. Wang Z, Li H, Li C, Yu Q, Shen J, De Saeger S (2014) Development and application of a quantitative fluorescence-based immunochromatographic assay for fumonisin b1 in maize. *J Agric Food Chem* 62(27):6294–6298. <https://doi.org/10.1021/jf5017219>
 13. Chen R, Li H, Zhang H, Zhang S, Shi W, Shen J, Wang Z (2013) Development of a lateral flow fluorescent microsphere immunoassay for the determination of sulfamethazine in milk. *Anal Bioanal Chem* 405(21):6783–6789. <https://doi.org/10.1007/s00216-013-7150-4>
 14. Torabi F, Mobini Far HR, Danielsson B, Khayyami M (2007) Development of a plasma panel test for detection of human myocardial proteins by capillary immunoassay. *Biosens Bioelectron* 22(7):1218–1223. <https://doi.org/10.1016/j.bios.2006.04.030>
 15. Chen A, Yang S (2015) Replacing antibodies with aptamers in lateral flow immunoassay. *Biosens Bioelectron* 71:230–242. <https://doi.org/10.1016/j.bios.2015.04.041>
 16. Wang L, Chen W, Ma W, Liu L, Ma W, Zhao Y, Zhu Y, Xu L, Kuang H, Xu C (2011) Fluorescent strip sensor for rapid determination of toxins. *Chem Commun (Camb)* 47(5):1574–1576. <https://doi.org/10.1039/c0cc04032k>
 17. Mao X, Ma Y, Zhang A, Zhang L, Zeng L, Liu G (2009) Disposable nucleic acid biosensors based on gold nanoparticle probes and lateral flow strip. *Anal Chem* 81(4):1660–1668. <https://doi.org/10.1021/ac8024653>
 18. Darwish NT, Sekaran SD, Khor SM (2018) Point-of-care tests: a review of advances in the emerging diagnostic tools for dengue virus infection. *Sensors Actuators B Chem* 255:3316–3331. <https://doi.org/10.1016/j.snb.2017.09.159>
 19. Sajid M, Kawde A-N, Daud M (2015) Designs, formats and applications of lateral flow assay: a literature review. *J Saudi Chem Soc* 19(6):689–705. <https://doi.org/10.1016/j.jscs.2014.09.001>
 20. Cheng S, Yang Y, Ni X, Peng J, Lai W (2017) Fluorescent microspheres lateral flow assay for sensitive detection of the milk allergen casein. *Food Agric Immunol* 28(6):1017–1028. <https://doi.org/10.1080/09540105.2017.1325841>
 21. Zhang X, Wen K, Wang Z, Jiang H, Beier RC, Shen J (2016) An ultra-sensitive monoclonal antibody-based fluorescent microsphere immunochromatographic test strip assay for detecting aflatoxin M 1 in milk. *Food Control* 60(2):588–595. <https://doi.org/10.1016/j.foodcont.2015.08.040>
 22. Gui C, Wang K, Li C, Dai X, Cui D (2014) A CCD-based reader combined with CdS quantum dot-labeled lateral flow strips for ultrasensitive quantitative detection of CagA. *Nanoscale Res Lett* 9(1):1–8. <https://doi.org/10.1186/1556-276X-9-57>
 23. Zeng N, You Y, Xie L, Zhang H, Ye L, Hong W, Li Y, Zeng N, You Y, Xie L (2017) A new imaged-based quantitative reader for the gold immunochromatographic assay. *Optik* 152:92–99. <https://doi.org/10.1016/j.ijleo.2017.09.109>
 24. Hohenstein J, O'Dell D, Mumane EL, Lu Z, Erickson D, Gay G (2017) Enhancing the usability of an optical reader system to support point-of-care rapid diagnostic testing: an iterative design approach. *JHF* 4(4):e29. <https://doi.org/10.2196/humanfactors.8621>
 25. Lee S, Kim G, Moon J (2013) Performance improvement of the one-dot lateral flow immunoassay for aflatoxin b1 by using a smartphone-based reading system. *Sensors* 13(4):5109–5116. <https://doi.org/10.3390/s130405109>
 26. Sefah K, Shangguan D, Xiong X, O'Donoghue MB, Tan W (2010) Development of DNA aptamers using Cell-SELEX. *Nat Protoc* 5(6):1169–1185. <https://doi.org/10.1038/nprot.2010.66>
 27. Xiao P, Lv X, Wang S, Iqbal J, Qing H, Li Q, Deng Y (2013) An aptamer-based trypsin reactor for on-line protein digestion with electrospray ionization tandem mass spectrometry. *Anal Biochem* 441(2):123–132. <https://doi.org/10.1016/j.ab.2013.06.012>
 28. Fialová M, Kypr J, Vorlíčková M (2006) The thrombin binding aptamer GGTGGTGTGGTTGG forms a bimolecular guanine tetraplex. *Biochem Biophys Res Commun* 344(1):50–54. <https://doi.org/10.1016/j.bbrc.2006.03.144>
 29. Vianini E, Palumbo M, Gatto B (2001) In vitro selection of DNA aptamers that bind L-tyrosinamide. *Bioorg Med Chem* 9(10):2543–2548. [https://doi.org/10.1016/S0968-0896\(01\)00054-2](https://doi.org/10.1016/S0968-0896(01)00054-2)
 30. Li S, Huo Y, Tian H, Zhang Q, Lv Y, Hao Z (2015) In vitro selection and characterization of deoxyribonucleic acid aptamers against connective tissue growth factor. *Biochem Biophys Res Commun* 457(4):640–646. <https://doi.org/10.1016/j.bbrc.2015.01.041>
 31. Ha NR, Lee SC, Hyun JW, Yoon MY (2016) Development of inhibitory ssDNA aptamers for the FtsZ cell division protein from citrus canker phytopathogen. *Process Biochem* 51(1):24–33. <https://doi.org/10.1016/j.procbio.2015.11.008>
 32. Di Nardo F, Anfossi L, Giovannoli C, Passini C, Gofman VV, Goryacheva IY, Baggiani C (2016) A fluorescent immunochromatographic strip test using Quantum Dots for fumonisins detection. *Talanta* 150:463–468. <https://doi.org/10.1016/j.talanta.2015.12.072>
 33. Liu M, Zeng LF, Yang YJ, Hu LM, Lai WH (2017) Fluorescent microsphere immunochromatographic assays for detecting bone alkaline phosphatase based on biolayer interferometry-selected antibody. *RSC Adv* 7(52):32952–32959. <https://doi.org/10.1039/C7RA03756B>